

Scalar Lattices and Probabilistic Shaping for Dithered Wyner-Ziv Quantization

M. Yusuf Şener^{*†}, Gerhard Kramer^{*}, Shlomo Shamai (Shitz)[‡], and Wen Xu[†]

^{*}School of Computation, Information and Technology, Technical University of Munich, 80333 Munich, Germany

[†]Munich Research Center, Huawei Technologies Duesseldorf GmbH, 80992 Munich, Germany

[‡]Dept. of Electrical and Computer Engineering, Technion—Israel Institute of Technology, Haifa 3200003, Israel
yusuf.sener@tum.de, gerhard.kramer@tum.de, sshlomo@ee.technion.ac.il, wen.xu@ieee.org

Abstract—Scalar lattice quantization with a modulo operator, dithering, and probabilistic shaping is applied to the Wyner-Ziv (WZ) problem with a Gaussian source and mean square error distortion. The method achieves the WZ rate-distortion pairs. The analysis is similar to that for dirty paper coding but requires additional steps to bound the distortion because the modulo shift is correlated with the source noise. The results extend to vector sources by reverse waterfilling on the spectrum of the covariance matrix of the source noise. Simulations with short polar codes illustrate the performance and compare with scalar quantizers and polar coded quantization without dithering.

I. INTRODUCTION

Optimal lossy source coding with side information at the decoder combines Shannon coding [1], [2] with Slepian-Wolf binning [3]. The best rate-distortion (RD) pairs are specified by the Wyner-Ziv (WZ) RD function [4], [5]; see [6, Ch. 15]. We study WZ coding for Gaussian vector sources and mean square error distortion; see [7]–[15].

WZ coding for real-valued sources can be implemented with multi-dimensional nested lattices [16]–[20]. Such lattices are helpful for many problems, e.g., dirty paper (DP) coding [21] and Gaussian networks [18, Ch. 12]. However, the high-dimensional modulo operations of [17] can be challenging to implement. Scalar shaping lattices are treated in [18, Ch. 6 & 9] but separated from quantization, and thus suboptimal.

A second approach applies nested linear codes directly to the DP and WZ problems. Polar codes [22] are well-suited because they enable practical joint coding and shaping [23]–[25] and inherently permit multilevel coding [26]; cf. [27]–[30]. One can approximate optimal coding densities using amplitude shift keying (ASK) for DP coding or, similarly, an equally-spaced scalar quantizer for WZ coding [31]–[44]. Multilevel binary polar codes are called polar coded modulation (PCM) in [26], and polar lattices in [32]–[36] for ASK. For quantization, we call such methods polar coded quantization (PCQ).

A third approach [45]–[47] uses scalar lattices, a modulo operator, and dithering. The primary purpose of this paper is to show this structure achieves the WZ curve. The proof is similar to [46] but requires additional steps because the modulo shift is correlated with the source noise; see Sec. III-D. We also treat vector sources by reverse waterfilling on the spectrum of the covariance matrix of the source noise; see [6, Fig. 10.7]. We remark dithering makes short block coding more challenging, see Sec. III-F, but has benefits for quantization and secrecy; see [18, Ch. 4], [48].

This paper is organized as follows. Sec. II reviews notation, theory for Gaussian vectors, and several RD functions. Sec. III describes a coding structure with a modulo operator and dithering. Simulations illustrate the performance; the abbreviations “PCQ” and “PCQmod” refer to polar coding without and with the dithered modulo structure, respectively. Sec. IV extends the results to vector sources. Sec. V concludes the paper.

II. PRELIMINARIES

A. Notation

Bold letters $\mathbf{x} = (x_1, \dots, x_d)^T$ refer to column vectors. Let $\mathbf{1}_d$ be the d -dimensional all-ones vector and I_d be the $d \times d$ identity matrix. Let $\mathbf{x} \circ \mathbf{y}$ be the Hadamard (entry-by-entry) product of \mathbf{x} and \mathbf{y} . Define the vector modulo operator

$$\mathbf{x} \bmod \mathbf{A} = \mathbf{x} - \mathbf{k} \circ \mathbf{A} \quad (1)$$

where \mathbf{A} has positive entries and k_i is the unique integer for which $x_i - k_i A_i \in [-A_i/2, A_i/2)$ for $i = 1, \dots, d$.

Upper- and lowercase letters usually refer to random variables (RVs) and their realizations, e.g., X is an RV, and x is its realization. P_X and p_X are a probability mass function and density, respectively. We remove subscripts if the argument is the lowercase of the RV, e.g., $p(x) = p_X(x)$. $\mathbb{E}[X]$ and the random vector $\mathbb{E}[X|Y]$ are the expectations of X without and with conditioning on Y , respectively. The corresponding covariance matrices are

$$Q_X = \mathbb{E}[(X - \mathbb{E}[X])(X - \mathbb{E}[X])^T] \quad (2)$$

$$Q_{X|Y} = \mathbb{E}[(X - \mathbb{E}[X|Y])(X - \mathbb{E}[X|Y])^T]. \quad (3)$$

For scalars, we write (2) and (3) as σ_x^2 and $\sigma_{x|y}^2$. The notation $h(X)$, $I(X; Y)$, $I(X; Y|Z)$ refers to the differential entropy of X and the mutual information of X and Y without and with conditioning on Z , respectively. We write $\mathbb{E}_q[f(X)] := \int_{\mathbb{R}} q(x)f(x) dx$ and $h_q(X) := \mathbb{E}_q[-\log q(X)]$.

B. Gaussian Vectors

We study jointly Gaussian X, Y , perhaps with different dimensions, and with zero mean and joint covariance matrix $Q_{X,Y}$. The conditional mean of X given Y is

$$\mathbb{E}[X|Y] = \mathbb{E}[XY^T] Q_Y^{-1} Y \quad (4)$$

assuming Q_Y is invertible. One may write

$$X = \mathbb{E}[X|Y] + Z \quad (5)$$

where \mathbf{Z} is independent of \mathbf{Y} and

$$Q_{\mathbf{Z}} = Q_{\mathbf{X}|\mathbf{Y}} = Q_{\mathbf{X}} - \mathbb{E}[\mathbf{X}\mathbf{Y}^T] Q_{\mathbf{Y}}^{-1} \mathbb{E}[\mathbf{Y}\mathbf{X}^T]. \quad (6)$$

Alternatively, we have

$$\mathbf{Y} = \mathbb{E}[\mathbf{Y}|\mathbf{X}] + \hat{\mathbf{Z}} \quad (7)$$

where $\hat{\mathbf{Z}}$ is independent of \mathbf{X} and (see (6))

$$Q_{\hat{\mathbf{Z}}} = Q_{\mathbf{Y}|\mathbf{X}} = Q_{\mathbf{Y}} - \mathbb{E}[\mathbf{Y}\mathbf{X}^T] Q_{\mathbf{X}}^{-1} \mathbb{E}[\mathbf{X}\mathbf{Y}^T] \quad (8)$$

assuming $Q_{\mathbf{X}}$ is invertible.

C. Rate-Distortion Theory

Consider a source that outputs a string $X^n = X_1, \dots, X_n$ of independent and identically distributed (i.i.d.) symbols. The lossy source coding problem has a non-negative real-valued distortion function $d(\cdot)$, an encoder mapping X^n to nR bits W , where R is the rate, and a decoder mapping W to a reconstruction $\hat{X}^n = \hat{X}_1, \dots, \hat{X}_n$. The goal is to design the encoder and decoder so the (random) empirical distortion

$$\Delta := \frac{1}{n} \sum_{i=1}^n d(X_i, \hat{X}_i) \quad (9)$$

satisfies $\mathbb{E}[\Delta] \leq \mathcal{D}$. We also study $\Pr[\Delta > \mathcal{D}]$, i.e., the probability of excess distortion for a specified \mathcal{D} .

The RD function is the infimum of R as a function of \mathcal{D} . Shannon [1], [2] showed that this function is

$$R(\mathcal{D}) = \min_{\mathbb{E}[d(X, \hat{X})] \leq \mathcal{D}} I(X; \hat{X}). \quad (10)$$

For example, if X is Gaussian and $d(x, \hat{x}) = (x - \hat{x})^2$, then

$$R(\mathcal{D}) = \begin{cases} \frac{1}{2} \log(\sigma_x^2 / \mathcal{D}), & 0 < \mathcal{D} < \sigma_x^2 \\ 0, & \mathcal{D} \geq \sigma_x^2. \end{cases} \quad (11)$$

For $0 < \mathcal{D} < \sigma_x^2$, the optimal “reverse” channel is

$$X = \hat{X} + Z \quad (12)$$

where \hat{X} and Z are independent and Gaussian with variances $\sigma_x^2 - \mathcal{D}$ and \mathcal{D} , respectively. Applying (7)-(8), we have

$$\hat{X} = \begin{cases} (1 - \mathcal{D}/\sigma_x^2)X + \hat{Z}, & 0 < \mathcal{D} < \sigma_x^2 \\ 0, & \mathcal{D} \geq \sigma_x^2 \end{cases} \quad (13)$$

where \hat{Z} is independent of X and $\sigma_{\hat{Z}}^2 = (1 - \mathcal{D}/\sigma_x^2)\mathcal{D}$.

D. Conditional Rate-Distortion Theory

Suppose the encoder and decoder have the side information $Y^n = Y_1, \dots, Y_n$ of i.i.d. symbols, i.e., the pairs (X_i, Y_i) are i.i.d. for $i = 1, \dots, n$. The conditional RD function is

$$R_{X|Y}(\mathcal{D}) = \min_{\mathbb{E}[d(X, \hat{X})] \leq \mathcal{D}} I(X; \hat{X}|Y). \quad (14)$$

For example, if X, Y are jointly Gaussian and the distortion function is $d(x, \hat{x}) = (x - \hat{x})^2$, then

$$R_{X|Y}(\mathcal{D}) = \begin{cases} \frac{1}{2} \log(\sigma_{x|y}^2 / \mathcal{D}), & 0 < \mathcal{D} < \sigma_{x|y}^2 \\ 0, & \mathcal{D} \geq \sigma_{x|y}^2. \end{cases} \quad (15)$$

More generally, suppose \mathbf{X} and \mathbf{Y} are jointly Gaussian and $d(\mathbf{x}, \hat{\mathbf{x}}) = \|\mathbf{x} - \hat{\mathbf{x}}\|^2$. Let $Q_{\mathbf{X}|\mathbf{Y}} = V\Lambda V^T$ be the eigenvalue

decomposition of $Q_{\mathbf{X}|\mathbf{Y}}$, where V is an orthogonal matrix and Λ is non-negative with diagonal entries λ_i , $i = 1, \dots, d$, where d is the dimension of \mathbf{X} . Then, if $\mathcal{D} \geq \sum_{i=1}^d \lambda_i$, we have $R_{\mathbf{X}|\mathbf{Y}}(\mathcal{D}) = 0$. Otherwise, we have (see [6, Ch. 10.3.3])

$$R_{\mathbf{X}|\mathbf{Y}}(\mathcal{D}) = \sum_{i: \lambda_i < \lambda} \frac{1}{2} \log(\lambda_i / \lambda) \quad (16)$$

where the reverse-waterfilling level $\lambda > 0$ is chosen so

$$\mathcal{D} = \sum_{i=1}^d \min(\lambda_i, \lambda). \quad (17)$$

The idea is that i -th encoder quantizes the i -th entry of

$$\mathbf{X}_V = V^T(\mathbf{X} - \mathbb{E}[\mathbf{X}|\mathbf{Y}]) \quad (18)$$

of variance λ_i ; observe that

$$Q_{\mathbf{X}_V} = V^T Q_{\mathbf{X}|\mathbf{Y}} V = \Lambda \quad (19)$$

so the entries of \mathbf{X}_V are uncorrelated, and hence independent. If λ_i is large, one transmits information about $X_{V,i}$; if λ_i is small, one transmits no information. Reverse waterfilling states that the boundary between “large” and “small” is λ , and the best descriptions have distortion λ if $\lambda < \lambda_i$. The reconstructions are as in (13), namely

$$\hat{X}_{V,i} = \begin{cases} (1 - \lambda/\lambda_i)X_{V,i} + \hat{Z}_i, & 0 < \lambda < \lambda_i \\ 0, & \lambda \geq \lambda_i \end{cases} \quad (20)$$

where the \hat{Z}_i , $i = 1, \dots, d$, and \mathbf{X}_V are mutually independent and $\sigma_{\hat{Z}_i}^2 = (1 - \lambda/\lambda_i)\lambda$. The output is $\hat{\mathbf{X}} = V\hat{\mathbf{X}}_V + \mathbb{E}[\mathbf{X}|\mathbf{Y}]$.

E. Wyner-Ziv Rates

The WZ extension of RD theory assumes the decoder, but not the encoder, has access to \mathbf{Y} . The RD function is now

$$R_{WZ}(\mathcal{D}) = \min_{\mathbb{E}[d(\mathbf{X}, \hat{\mathbf{X}})] \leq \mathcal{D}} (I(\mathbf{U}; \mathbf{X}) - I(\mathbf{U}; \mathbf{Y})) \quad (21)$$

where the minimization is over all \mathbf{U} such that $\mathbf{U} \leftrightarrow \mathbf{X} \leftrightarrow \mathbf{Y}$ forms a Markov chain, and all functions $f(\cdot)$ such that $\hat{\mathbf{X}} = f(\mathbf{U}, \mathbf{Y})$. The Markov chain relation gives

$$I(\mathbf{U}; \mathbf{X}) - I(\mathbf{U}; \mathbf{Y}) = I(\mathbf{U}; \mathbf{X}|\mathbf{Y}). \quad (22)$$

Remarkably, $R_{WZ}(\mathcal{D}) = R_{\mathbf{X}|\mathbf{Y}}(\mathcal{D})$ if \mathbf{X}, \mathbf{Y} are jointly Gaussian and $d(\mathbf{x}, \hat{\mathbf{x}}) = \|\mathbf{x} - \hat{\mathbf{x}}\|^2$, i.e., the RD function is the same as if the encoder also has \mathbf{Y} . For example, consider the scalar problem and choose $U = X + \tilde{Z}$ where \tilde{Z} is independent of (X, Y) . The best estimate of X is

$$\hat{X} = \mathbb{E}[X|U, Y] = \frac{\sigma_{x|y}^2 U + \sigma_{\tilde{Z}}^2 \mathbb{E}[X|Y]}{\sigma_{x|y}^2 + \sigma_{\tilde{Z}}^2}. \quad (23)$$

If $0 < \mathcal{D} < \sigma_{x|y}^2$, choose the description noise variance as

$$\sigma_{\tilde{Z}}^2 = \frac{\sigma_{x|y}^2 \mathcal{D}}{\sigma_{x|y}^2 - \mathcal{D}} \implies \mathcal{D} = \frac{\sigma_{x|y}^2 \sigma_{\tilde{Z}}^2}{\sigma_{x|y}^2 + \sigma_{\tilde{Z}}^2} \quad (24)$$

This choice gives $\mathbb{E}[(X - \hat{X})^2] = \mathcal{D}$ and

$$I(\mathbf{U}; \mathbf{X}) - I(\mathbf{U}; \mathbf{Y}) = \frac{1}{2} \log(\sigma_{x|y}^2 / \mathcal{D}). \quad (25)$$

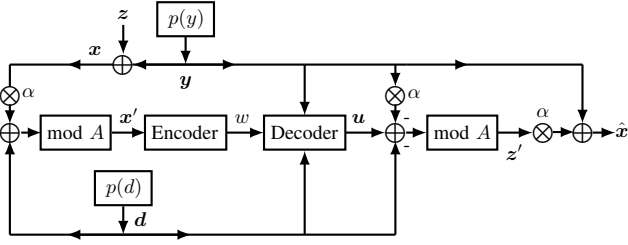


Fig. 1. WZ coding with a modulo operator and dithering.

III. SCALAR MODELS AND QUANTIZATION

Consider $X = Y + Z$ where Z is Gaussian and independent of Y , i.e., we have $\sigma_{x|y}^2 = \sigma_z^2$. Fig. 1 shows the WZ coding structure of [17, Sec. IV.A] but with scalar operations. The encoder and decoder share a dither D statistically independent of (X, Z) and uniformly distributed in $[-A/2, A/2)$. The inflation factor is $\alpha = \sqrt{1 - \sigma_d^2/\sigma_z^2}$, where σ_d^2 is a target distortion; cf. [17, p. 1260].

A. Model in a Finite Interval

We derive a model for the interval $[-A/2, A/2)$ by modifying steps in [17], [45]–[47]. The derived source is

$$(X', Y')^T = (\alpha(X, Y)^T + D \cdot \mathbf{1}_2) \bmod A \cdot \mathbf{1}_2. \quad (26)$$

The dither makes X' uniform over $[-A/2, A/2)$ and independent of X , and similarly for Y' and Y . The source X' is quantized via U with discrete alphabet \mathcal{U} . Using standard theory, the decoder can recover U if the rate satisfies

$$R = I(U; X') - I(U; Y') \quad (27)$$

where $U \leftrightarrow X' \leftrightarrow Y'$ forms a Markov chain; see (21).

Let σ_d^2 be a distortion parameter satisfying $0 < \sigma_d^2 < \sigma_z^2$. Define the encoder and decoder noise

$$\tilde{Z} = (U - X') \bmod A \quad (28)$$

$$Z' = (U - Y') \bmod A = (\tilde{Z} + \alpha Z) \bmod A \quad (29)$$

where U is selected based on X' only; see Sec. III-B below. Thus, $U \leftrightarrow X' \leftrightarrow Y'$ forms a Markov chain, as required.

The decoder puts out the reconstruction

$$\hat{X} = Y + \alpha Z' \quad (30)$$

Observe that $\hat{X} = \mathbb{E}[X|Y, Z']$ if $Z' = \tilde{Z} + \alpha Z$ is Gaussian and \tilde{Z} is independent of (Y, Z) and has variance σ_d^2 . Also, \hat{X} is a function of U and Y , as required.

B. Scalar Lattices and Probabilistic Shaping

Consider the equally spaced scalar quantizer with alphabet

$$\mathcal{U} = \left\{ -A/2 + (2k+1)\kappa \right\}_{k=0}^{M-1} \quad (31)$$

where $A \geq 0$ and $\kappa = A/(2M)$. We call this alphabet M -ASK to match [45]–[47]. Let $q(\tilde{z})$ be a density on $\tilde{z} \in [-A/2, A/2)$ and apply the probabilistic shaping

$$P(u|x') = \frac{q((u - x') \bmod A)}{\sum_{v \in \mathcal{U}} q((v - x') \bmod A)}, \quad u \in \mathcal{U}. \quad (32)$$

Observe that X', \tilde{Z} play the roles of S', X in [46], e.g., the continuously uniform X' induces a discrete uniform U . To see this, define $\tilde{x} = (u - x') \bmod A$ and

$$d(x) = 2\kappa \sum_{k=0}^{M-1} q((x + 2k\kappa) \bmod A). \quad (33)$$

We then have

$$P(u) = \int_{-A/2}^{A/2} \frac{1}{A} P(u|x') dx' = \int_{-A/2}^{A/2} \frac{1}{M} \frac{q(\tilde{x})}{d(\tilde{x})} d\tilde{x} \quad (34)$$

and $P(u) = 1/M$ for all u since (34) does not depend on u .

We claim U, \tilde{Z}, Z are mutually statistically independent and

$$p(\tilde{z}) = q(\tilde{z})/d(\tilde{z}), \quad \tilde{z} \in [-A/2, A/2). \quad (35)$$

To see this, let $x' = (u - \tilde{z}) \bmod A$. We have

$$\begin{aligned} p(\tilde{z}, z|u) &= p(x', z|u) \\ &\stackrel{(a)}{=} (p(x')P(u|x')/P(u)) p(z) \\ &\stackrel{(b)}{=} \frac{q(\tilde{z})}{d(\tilde{z})} p(z) \end{aligned} \quad (36)$$

where step (a) follows because (X', U) and Z are independent, and step (b) follows by $p(x') = 1/A$ and $P(u) = 1/M$.

C. Truncated Gaussian Shaping

We use truncated Gaussian shaping with (see [46, eq. (12)])

$$q(\tilde{z}) = \frac{e^{-\tilde{z}^2/(2\sigma_d^2)}}{c \cdot \sqrt{2\pi\sigma_d^2}}, \quad \tilde{z} \in [-A/2, A/2) \quad (37)$$

where $c = 1 - 2Q(A/(2\sigma_d))$. We compute (see [46, eq. (16)])

$$P_{q,\tilde{Z}} := \mathbb{E}_q[\tilde{Z}^2] = \sigma_d^2 \left[1 - \frac{Ae^{-A^2/(8\sigma_d^2)}}{c\sqrt{2\pi\sigma_d^2}} \right] \quad (38)$$

and (see [46, eq. (17)])

$$h_q(\tilde{Z}) = \frac{1}{2} \log(2\pi e \sigma_d^2 c^2) - \frac{1}{2} \left(1 - \frac{P_{q,\tilde{Z}}}{\sigma_d^2} \right). \quad (39)$$

Since $q(\cdot)$ is symmetric unimodal, by [47, eq. (20)] we have $d_{\min} \leq d(x) \leq d_{\max}$ where

$$d_{\min} = 1 - \frac{A}{M} q(0), \quad d_{\max} = 1 + \frac{A}{M} q(0). \quad (40)$$

D. Distortion

To bound the distortion, consider

$$X - \hat{X} = Z - \alpha Z'. \quad (41)$$

The modulo operator cannot increase the second moment, so

$$\begin{aligned} \mathbb{E}[(Z')^2] &\leq \mathbb{E}[(\tilde{Z} + \alpha Z)^2] \\ &\stackrel{(a)}{\leq} \frac{1}{d_{\min}} \mathbb{E}_q[\tilde{Z}^2] + \alpha^2 \sigma_z^2 \\ &= \sigma_z^2 + (P_{q,\tilde{Z}}/d_{\min} - \sigma_d^2) \end{aligned} \quad (42)$$

where step (a) follows by $p(\tilde{z}) \leq q(\tilde{z})/d_{\min}$ if M is sufficiently large so $d_{\min} > 0$; see (35) and (40). We further have

$$\begin{aligned} \mathbb{E}[ZZ'] &= \mathbb{E}[Z(\tilde{Z} + \alpha Z - IA)] \\ &= \alpha \sigma_z^2 - A \mathbb{E}[IZ] \end{aligned} \quad (43)$$

where we used the independence of Z and \tilde{Z} , and I is the RV taking on the modulo shift values i . We thus have

$$\begin{aligned} \mathbb{E} \left[(X - \hat{X})^2 \right] &= \sigma_z^2 - 2\alpha \mathbb{E}[ZZ'] + \alpha^2 \mathbb{E}[(Z')^2] \\ &\stackrel{(a)}{\leq} \sigma_d^2 + 2\alpha A \mathbb{E}[IZ] + \alpha^2 (P_{q,\tilde{Z}}/d_{\min} - \sigma_d^2) \end{aligned} \quad (44)$$

where step (a) follows by (42) and (43).

We bound the term $2\alpha A \mathbb{E}[IZ]$. Define the intervals

$$\mathcal{I}_k = [kA - A/2, kA + A/2], \quad k \in \mathbb{Z} \quad (45)$$

and let $Z'' = \tilde{Z} + \alpha Z$. By symmetry, we have

$$\mathbb{E}[Z|Z'' \in \mathcal{I}_{(-k)}] = -\mathbb{E}[Z|Z'' \in \mathcal{I}_k]. \quad (46)$$

The law of total expectation thus gives

$$\begin{aligned} 2\alpha A \mathbb{E}[IZ] &= 4\alpha \sum_{k \geq 1} \Pr[Z'' \in \mathcal{I}_k] \underbrace{kA \mathbb{E}[Z|Z'' \in \mathcal{I}_k]}_{\leq kA/\alpha} \\ &\leq 4 \int_{A/2}^{\infty} p_{Z''}(x) \cdot (x + A/2)^2 dx \end{aligned} \quad (47)$$

where

$$\begin{aligned} p_{Z''}(x) &= p_{\tilde{Z}} * p_{\alpha Z}(x) = \int_{-A/2}^{A/2} \frac{q(y)}{d(y)} p_{\alpha Z}(x - y) dy \\ &\stackrel{(a)}{\leq} \frac{e^{-x^2/(2\sigma_z^2)}}{c d_{\min} \cdot \sqrt{2\pi\sigma_z^2}} \end{aligned} \quad (48)$$

and where step (a) follows by extending the domain of $q(\cdot)$ in (37) to all reals. We may thus bound (47) as

$$\begin{aligned} 2\alpha A \mathbb{E}[IZ] &\leq \frac{4}{c d_{\min}} \int_{A/2}^{\infty} \frac{e^{-x^2/(2\sigma_z^2)}}{\sqrt{2\pi\sigma_z^2}} \cdot (x + A/2)^2 dx \\ &= \frac{4}{c d_{\min}} \left[\frac{3A\sigma_z^2}{2} \cdot \frac{e^{-A^2/(8\sigma_z^2)}}{\sqrt{2\pi\sigma_z^2}} + \left(\sigma_z^2 + \frac{A^2}{4} \right) Q\left(\frac{A}{2\sigma_z}\right) \right]. \end{aligned} \quad (49)$$

The right-hand side of (49) vanishes as $A \rightarrow \infty$.

E. Source Coding Rate

For the rate R , similar to [46], we have

$$I(U; X') = h(X') - h(\tilde{Z}|U) = \log A - h(\tilde{Z}) \quad (50)$$

$$I(U; Y') = h(Y') - h(Z'|U) = \log A - h(Z') \quad (51)$$

where we used the independence of U , \tilde{Z} , Z . We may use [47, eq. (25)] to lower bound $h(\tilde{Z})$ and (42) gives

$$h(Z') \leq \frac{1}{2} \log \left(2\pi e (\sigma_z^2 + P_{q,\tilde{Z}}/d_{\min} - \sigma_d^2) \right). \quad (52)$$

We proceed as in [46], [47] and first take the limit $M \rightarrow \infty$ to obtain $d(\tilde{z}) \rightarrow 1$ and $p(\tilde{z}) \rightarrow q(\tilde{z})$ for $\tilde{z} \in [-A/2, A/2]$. We next take the limit $A \rightarrow \infty$ to obtain $p(\tilde{z}) \rightarrow \mathcal{N}(0; \sigma_d^2)$ and $p(z') \rightarrow \mathcal{N}(0; \sigma_z^2)$. We therefore obtain the WZ rate.

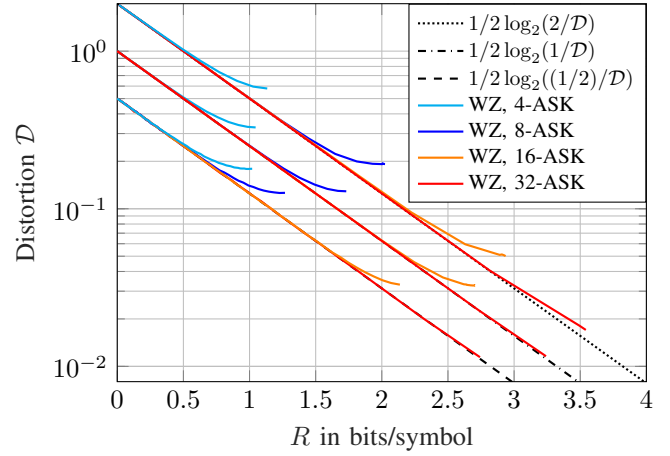


Fig. 2. RD curves for $(\sigma_y^2, \sigma_z^2) = (0, 2), (1, 1), (3/2, 1/2)$ and $\sigma_x^2 = 2$. The target rates are $R = \frac{1}{2} \log(\sigma_z^2/D)$.

F. Simulations with Short Polar Codes

Fig. 2 shows RD curves for $M = 4, 8, 16, 32$. The 4-ASK curves have $A = 10, 8, 6$ for $\sigma_y^2 = 0, 1, 3/2$, respectively. The 8-ASK and 16-ASK curves have $A = 12, 10, 10$, and the 32-ASK curves have $A = 14, 12, 10$. The figure illustrates that increasing M and A achieves the WZ curve.

Consider $R = 1$ and 8-ASK with natural labeling. We use multilevel coding with $L = \log_2 M$ levels, where levels 1 to L carry successively more significant bits. Each level has one 5G NR polar code of length 256. The encoder and decoder use successive cancellation list decoding [49] with list size 8 and list passing across levels [50], [51]. The most reliable polar subchannels of each level are assigned shaping bits, the next most reliable information bits, and the rest frozen bits. We optimized A , σ_d^2 , and the numbers of message and shaping bits across the polar subchannels to minimize $\mathbb{E}[D]$.

We study two sources; Fig. 3 plots $\Pr[\Delta > D]$.

- Source 1: $\sigma_y^2 = 0$, $\sigma_z^2 = \sigma_x^2 = 2$, $\mathbb{E}[\Delta] \geq 0.5$
 - one-bit scalar quantizer: $\mathbb{E}[\Delta] = 0.727$
 - PCQ: $\mathbb{E}[\Delta] = 0.614$ for ASK spacing 0.6
 - PCQmod: $\mathbb{E}[\Delta] = 0.713$ for $A/M = 1.5$
- Source 2: $\sigma_y^2 = \sigma_z^2 = 1$, $\mathbb{E}[\Delta] \geq 0.25$
 - one-bit scalar quantizer: $\mathbb{E}[\Delta] = 0.519$
 - PCQ: $\mathbb{E}[\Delta] = 0.351$ for ASK spacing 0.8
 - PCQmod: $\mathbb{E}[\Delta] = 0.357$ for $A/M = 1.25$

Fig. 3 shows PCQ outperforms PCQmod, notably for $\sigma_y^2 = 0$ where PCQ can use a (relatively) fine ASK spacing with few shaping bits. PCQmod requires coarser ASK spacing and more shaping bits because A must be sufficiently large to limit the number of modulo shifts, while the dither makes $I(U; Y')$ grow as $\log A$ even if $Y = 0$; see (51). Fig. 3 also shows PCQ and PCQmod perform similarly as σ_y^2 increases; this is because WZ coding requires shaping bits for both methods, as represented by $I(U; Y)$ for PCQ and $I(U; Y')$ for PCQmod. We remark dithering benefits quantization and secrecy by making (X', M) independent of X [18, Ch. 4].

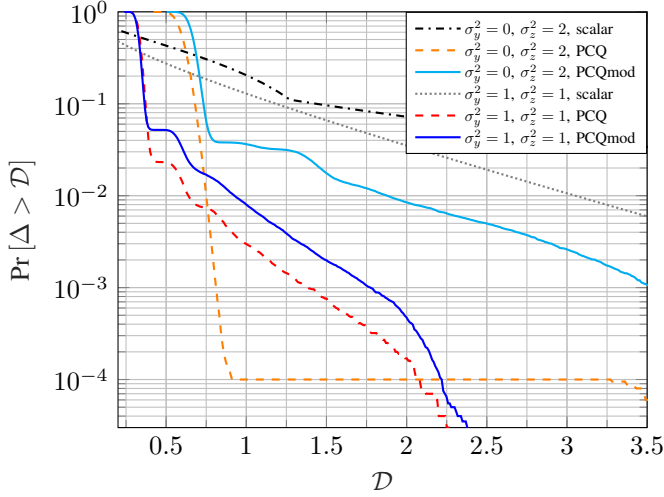


Fig. 3. $\Pr[\Delta > D]$ for $\sigma_x^2 = 2$, $R = 1$, 8-ASK, and $n = 256$.

IV. VECTOR MODELS AND QUANTIZATION

Consider the vectors \mathbf{X}, \mathbf{Y} . We re-define (see (18))

$$\mathbf{X}_V := V^T \mathbf{X} = V^T \mathbf{E}[\mathbf{X}|\mathbf{Y}] + V^T \mathbf{Z} \quad (53)$$

because the encoder does not have \mathbf{Y} . Let $\mathbf{Y}_V = V^T \mathbf{E}[\mathbf{X}|\mathbf{Y}]$ so we have (see (19))

$$Q_{\mathbf{X}_V|\mathbf{Y}} = Q_{\mathbf{X}_V|\mathbf{Y}_V} = Q_{V^T \mathbf{Z}} = \Lambda. \quad (54)$$

Thus, the $X_{V,1}, \dots, X_{V,d}$ are independent given \mathbf{Y} or \mathbf{Y}_V . Moreover, if \mathbf{v}_i^T is the i -th row of V^T , we have

$$\mathbf{E}[X_{V,i}|\mathbf{Y}] = \mathbf{v}_i^T \mathbf{E}[\mathbf{X}\mathbf{Y}^T] Q_Y^{-1} \mathbf{Y} = Y_{V,i} \quad (55)$$

and therefore $X_{V,i} \leftrightarrow Y_{V,i} \leftrightarrow \mathbf{Y}$ forms a Markov chain.

For coding, mimic (23)–(25) and choose

$$U_i = X_{V,i} + \tilde{Z}_i, \quad i = 1, \dots, d \quad (56)$$

where $\tilde{Z}_1, \dots, \tilde{Z}_n, (\mathbf{X}, \mathbf{Y})$ are mutually independent. We have the Markov chains $U_i \leftrightarrow X_{V,i} \leftrightarrow Y_{V,i} \leftrightarrow \mathbf{Y}$ and (22) gives

$$R = I(\mathbf{U}; \mathbf{X}|\mathbf{Y}) = \sum_{i=1}^d I(U_i; X_{V,i}|\mathbf{Y}_{V,i}) \quad (57)$$

where $X_{V,i} - \mathbf{E}[X_{V,i}|\mathbf{Y}_{V,i}]$ has variance λ_i . We describe $X_{V,i}$ with the reverse waterfilling level λ as in Sec. II-E to obtain the $\hat{X}_{V,i}$ in (20). Thus, the distortions for $i = 1, \dots, d$ are $\min(\lambda_i, \lambda)$ and the sub-channel rates are

$$R_i = I(U_i; X_{V,i}|\mathbf{Y}_{V,i}) = \begin{cases} \frac{1}{2} \log(\lambda_i/\lambda), & \lambda < \lambda_i \\ 0, & \lambda \geq \lambda_i \end{cases} \quad (58)$$

A. Simulations with Short Polar Codes

The expression (57) suggests using the scalar structure of Sec. III in parallel with different A_i, M_i for each source pair $X_{V,i}, Y_{V,i}$, $i = 1, \dots, d$. For example, consider $d = 2$ and

$$Q_Z = \frac{1}{4} \begin{pmatrix} 3 & 1 \\ 1 & 3 \end{pmatrix} = V^T \Lambda V \quad (59)$$

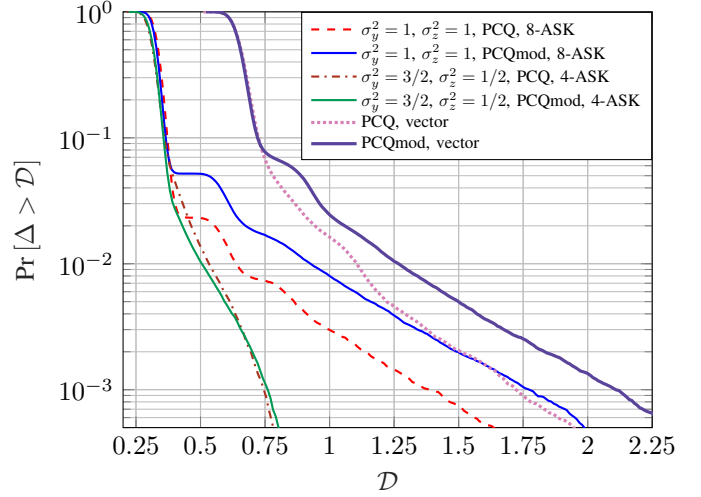


Fig. 4. $\Pr[\Delta > D]$ for a vector source, $R = 3/2$, and $n = 256$.

where

$$\Lambda = \begin{pmatrix} 1 & 0 \\ 0 & 1/2 \end{pmatrix}, \quad V = \frac{1}{\sqrt{2}} \begin{pmatrix} 1 & 1 \\ 1 & -1 \end{pmatrix}. \quad (60)$$

Suppose $\mathbf{E}[Y_{V,1}^2] = 1$ and $\mathbf{E}[Y_{V,2}^2] = 3/2$. The rate $R = 3/2$ is achieved with $\lambda = 1/4$ and $(R_1, R_2) = (1, 1/2)$, i.e., both sub-channel encoders are active with target distortion $\lambda = 1/4$ and $\mathbf{E}[\Delta] \geq 2\lambda = 1/2$. We study 8-ASK for $R_1 = 1$ and 4-ASK for $R_2 = 1/2$. Let Δ_1 and Δ_2 be the corresponding distortion RVs. We have $R = R_1 + R_2$ and $\Delta = \Delta_1 + \Delta_2$. Fig. 4 plots the $\Pr[\Delta > D]$ curves; cf. Fig. 3.

- Source 1: $\sigma_y^2 = \sigma_z^2 = 1$, $R_1 = 1$, $\mathbf{E}[\Delta_1] \geq 0.25$
 - PCQ: $\mathbf{E}[\Delta_1] = 0.351$ for ASK spacing 0.8
 - PCQmod: $\mathbf{E}[\Delta_1] = 0.357$ for $A/M = 1.25$
- Source 2: $\sigma_y^2 = 3/2$, $\sigma_z^2 = 1/2$, $R_2 = 1/2$, $\mathbf{E}[\Delta_2] \geq 0.25$
 - PCQ: $\mathbf{E}[\Delta_2] = 0.327$ for ASK spacing 1.5
 - PCQmod: $\mathbf{E}[\Delta_2] = 0.328$ for $A/M = 1.5$

The vector source has $R = 3/2$ and $\mathbf{E}[\Delta] = \mathbf{E}[\Delta_1] + \mathbf{E}[\Delta_2]$.

V. CONCLUSIONS

We showed PCQmod achieves the WZ curve for Gaussian vector sources and mean square error distortion. Vector coding uses a parallel structure motivated by (57) with the transformed source $\mathbf{X}_V, \mathbf{Y}_V$. Simulations with short polar codes show that PCQ outperforms PCQmod without side information. PCQ and PCQmod perform similarly as the side information becomes prominent, and PCQmod has the benefits of dithering.

Future work could replace the decoder's modulo operator with a scalar minimum mean square error estimator. One could also study different dynamic ranges of dithering, both with and without modulo operators, and how dithering provides robustness for realistic sources, i.e., non-Gaussian \mathbf{X}, \mathbf{Y} .

VI. ACKNOWLEDGEMENTS

This work was supported by the German Research Foundation (DFG) via the German-Israeli Project Cooperation (DIP) under projects KR 3517/13-1 and SH 1937/1-1.

REFERENCES

- [1] C. E. Shannon, "A mathematical theory of communication," *Bell Sys. Techn. J.*, vol. 27, pp. 379–423 and 623–656, 1948, Reprinted in *Claude Elwood Shannon: Collected Papers*, pp. 5–83, (N.J.A. Sloane and A.D. Wyner, eds.) Piscataway: IEEE Press, 1993.
- [2] —, "Coding theorems for a discrete source with a fidelity criterion," in *IRE Int. Conv. Rec.*, 1959, pp. 142–163, Reprinted in *Claude Elwood Shannon: Collected Papers*, pp. 325–350, (N.J.A. Sloane and A.D. Wyner, eds.) Piscataway: IEEE Press, 1993.
- [3] D. Slepian and J. Wolf, "Noiseless coding of correlated information sources," *IEEE Trans. Inf. Theory*, vol. 19, no. 4, pp. 471–480, 1973.
- [4] A. Wyner and J. Ziv, "The rate-distortion function for source coding with side information at the decoder," *IEEE Trans. Inf. Theory*, vol. 22, no. 1, pp. 1–10, 1976.
- [5] A. Wyner, "The rate-distortion function for source coding with side information at the decoder-II: General sources," *Inf. Control*, vol. 38, no. 1, pp. 60–80, 1978.
- [6] T. M. Cover and J. A. Thomas, *Elements of Information Theory*, 2nd ed. New York: John Wiley & Sons, 2006.
- [7] R. McDonald and P. Schultheiss, "Information rates of Gaussian signals under criteria constraining the error spectrum," *Proc. IEEE*, vol. 52, no. 4, pp. 415–416, 1964.
- [8] Y. Oohama, "Gaussian multiterminal source coding," *IEEE Trans. Inf. Theory*, vol. 43, no. 6, pp. 1912–1923, 1997.
- [9] R. Puri and K. Ramchandran, "PRISM: a new robust video coding architecture based on distributed compression principles," in *Allerton Conf. Commun. Control, Comp.*, Allerton, IL, USA, 2002, pp. 586–595.
- [10] Y. Oohama, "Rate-distortion theory for Gaussian multiterminal source coding systems with several side informations at the decoder," *IEEE Trans. Inf. Theory*, vol. 51, no. 7, pp. 2577–2593, 2005.
- [11] M. Gastpar, P. L. Dragotti, and M. Vetterli, "The distributed Karhunen-Loève transform," *IEEE Trans. Inf. Theory*, vol. 52, no. 12, pp. 5177–5196, 2006.
- [12] C. Tian and J. Chen, "Remote vector Gaussian source coding with decoder side information under mutual information and distortion constraints," *IEEE Trans. Inf. Theory*, vol. 55, no. 10, pp. 4676–4680, 2009.
- [13] J. Wang and J. Chen, "Vector Gaussian multiterminal source coding," *IEEE Trans. Inf. Theory*, vol. 60, no. 9, pp. 5533–5552, 2014.
- [14] A. Zahedi, J. Østergaard, S. H. Jensen, P. Naylor, and S. Bech, "Distributed remote vector Gaussian source coding with covariance distortion constraints," in *IEEE Int. Symp. Inf. Theory*, Honolulu, HI, USA, 2014, pp. 586–590.
- [15] M. Gkagkos and C. D. Charalambous, "Structural properties of the Wyner-Ziv rate distortion function: Applications for multivariate Gaussian sources," *Entropy*, vol. 26, no. 4, p. 306, 2024.
- [16] R. Zamir and S. Shamai, "Nested linear/lattice codes for Wyner-Ziv encoding," in *Inf. Theory Workshop*, Killarney, Ireland, 1998, pp. 92–93.
- [17] R. Zamir, S. Shamai, and U. Erez, "Nested linear/lattice codes for structured multiterminal binning," *IEEE Trans. Inf. Theory*, vol. 48, no. 6, pp. 1250–1276, 2002.
- [18] R. Zamir, *Lattice Coding for Signals and Networks*. Cambridge, U.K.: Cambridge Univ. Press, 2014.
- [19] A. Campello, D. Dadush, and C. Ling, "AWGN-goodness is enough: Capacity-achieving lattice codes based on dithered probabilistic shaping," *IEEE Trans. Inf. Theory*, vol. 65, no. 3, pp. 1961–1971, 2019.
- [20] H. Dongbo, H. Gang, X. Yonggang, and Y. Hongsheng, "Nested lattice coding with algebraic encoding and geometric decoding," *IEEE Access*, vol. 9, pp. 11 598–11 609, 2021.
- [21] M. Costa, "Writing on dirty paper," *IEEE Trans. Inf. Theory*, vol. 29, no. 3, pp. 439–441, 1983.
- [22] E. Arikian, "Channel polarization: A method for constructing capacity-achieving codes for symmetric binary-input memoryless channels," *IEEE Trans. Inf. Theory*, vol. 55, no. 7, pp. 3051–3073, 2009.
- [23] S. B. Korada and R. L. Urbanke, "Polar codes are optimal for lossy source coding," *IEEE Trans. Inf. Theory*, vol. 56, no. 4, pp. 1751–1768, 2010.
- [24] D. Sutter, J. M. Renes, F. Dupuis, and R. Renner, "Achieving the capacity of any DMC using only polar codes," in *IEEE Inf. Theory Workshop*, Lausanne, Switzerland, 2012, pp. 114–118.
- [25] J. Honda and H. Yamamoto, "Polar coding without alphabet extension for asymmetric models," *IEEE Trans. Inf. Theory*, vol. 59, no. 12, pp. 7829–7838, 2013.
- [26] M. Seidl, A. Schenk, C. Stierstorfer, and J. B. Huber, "Polar-coded modulation," *IEEE Trans. Commun.*, vol. 61, no. 10, pp. 4108–4119, 2013.
- [27] H. Imai and S. Hirakawa, "A new multilevel coding method using error-correcting codes," *IEEE Trans. Inf. Theory*, vol. 23, no. 3, pp. 371–377, 1977.
- [28] U. Wachsmann, R. F. Fischer, and J. B. Huber, "Multilevel codes: theoretical concepts and practical design rules," *IEEE Trans. Inf. Theory*, vol. 45, no. 5, pp. 1361–1391, 1999.
- [29] G. Böcherer, T. Prinz, P. Yuan, and F. Steiner, "Efficient polar code construction for higher-order modulation," in *IEEE Wireless Commun. Networking Conf. Workshops*, San Francisco, CA, USA, 2017, pp. 1–6.
- [30] T. Prinz, P. Yuan, G. Böcherer, F. Steiner, O. İşcan, R. Böhnke, and W. Xu, "Polar coded probabilistic amplitude shaping for short packets," in *IEEE Int. Workshop Signal Proc. Advances in Wireless Commun.*, Sapporo, Japan, 2017, pp. 1–5.
- [31] S. Eghbalian-Arani and H. Behrooz, "Polar codes for a quadratic-Gaussian Wyner-Ziv problem," in *Int. Symp. Wireless Commun. Sys.*, Ilmenau, Germany, 2013, pp. 1–5.
- [32] L. Liu and C. Ling, "Polar codes and polar lattices for independent fading channels," *IEEE Trans. Commun.*, vol. 64, no. 12, pp. 4923–4935, 2016.
- [33] L. Liu, Y. Yan, C. Ling, and X. Wu, "Construction of capacity-achieving lattice codes: Polar lattices," *IEEE Trans. Commun.*, vol. 67, no. 2, pp. 915–928, 2019.
- [34] L. Liu, J. Shi, and C. Ling, "Polar lattices for lossy compression," *IEEE Trans. Inf. Theory*, vol. 67, no. 9, pp. 6140–6163, 2021.
- [35] L. Liu, S. Lyu, C. Ling, and B. Bai, "On the equivalence between probabilistic shaping and geometric shaping: A polar lattice perspective," in *IEEE Int. Symp. Inf. Theory*, Athens, Greece, 2024, pp. 2174–2179.
- [36] S. Jha, "Universal Gaussian quantization with side-information using polar lattices," *IEEE J. Sel. Areas Inf. Theory*, vol. 3, no. 4, pp. 639–650, 2022.
- [37] M. Mondelli, S. H. Hassani, and R. L. Urbanke, "How to achieve the capacity of asymmetric channels," *IEEE Trans. Inf. Theory*, vol. 64, no. 5, pp. 3371–3393, 2018.
- [38] O. İşcan, R. Böhnke, and W. Xu, "Shaped polar codes for higher order modulation," *IEEE Commun. Lett.*, vol. 22, no. 2, pp. 252–255, 2018.
- [39] —, "Probabilistic shaping using 5G New Radio polar codes," *IEEE Access*, vol. 7, pp. 22 579–22 587, 2019.
- [40] —, "Sign-bit shaping using polar codes," *Trans. Emerging Telecommun. Technol.*, vol. 31, no. 10, p. e4058, 2020.
- [41] T. Wiegart, F. Steiner, P. Schulte, and P. Yuan, "Shaped on-off keying using polar codes," *IEEE Commun. Lett.*, vol. 23, no. 11, pp. 1922–1926, 2019.
- [42] R. Böhnke, O. İşcan, and W. Xu, "Multi-level distribution matching," *IEEE Commun. Lett.*, vol. 24, no. 9, pp. 2015–2019, 2020.
- [43] C. Runge, T. Wiegart, D. Lentner, and T. Prinz, "Multilevel binary polar-coded modulation achieving the capacity of asymmetric channels," in *IEEE Int. Symp. Inf. Theory*, Espoo, Finland, 2022, pp. 2595–2600.
- [44] C. Runge and G. Kramer, "Time-shifted alternating Gelfand-Pinsker coding for broadcast channels," in *IEEE Int. Symp. Inf. Theory*, Athens, Greece, 2024, pp. 1700–1705.
- [45] M. Y. Şener, R. Böhnke, W. Xu, and G. Kramer, "Dirty paper coding based on polar codes and probabilistic shaping," *IEEE Commun. Lett.*, vol. 25, no. 12, pp. 3810–3813, 2021.
- [46] —, "Achieving the dirty paper channel capacity with scalar lattices and probabilistic shaping," *IEEE Commun. Lett.*, vol. 28, no. 1, pp. 29–33, 2024.
- [47] M. Y. Şener, G. Kramer, S. Shamai Shitz, R. Böhnke, and W. Xu, "Achieving Gaussian vector broadcast channel capacity with scalar lattices," in *IEEE Int. Symp. Inf. Theory*, Athens, Greece, 2024, pp. 1706–1711.
- [48] S. P. Lipshitz, R. A. Wannamaker, and J. Vanderkooy, "Quantization and dither: A theoretical survey," *J. Audio. Eng. Soc.*, vol. 40, no. 5, pp. 355–375, 1992.
- [49] I. Tal and A. Vardy, "List decoding of polar codes," *IEEE Trans. Inf. Theory*, vol. 61, no. 5, pp. 2213–2226, 2015.
- [50] T. Prinz and P. Yuan, "Successive cancellation list decoding of BMERA codes with application to higher-order modulation," in *IEEE Int. Symp. Turbo Codes Iter. Inf. Proc.*, Hong Kong, China, 2018, pp. 1–5.
- [51] L. Karakchieva and P. Trifonov, "Joint list multistage decoding with sphere detection for polar coded SCMA systems," in *Int. ITG Conf. Sys., Commun. Coding*, Rostock, Germany, 2019, pp. 1–6.